Laser and Particle Beams (2009), *27*, 629–634.

doi:10.1017/S0263034609990371

Efficient acceleration of a small dense plasma pellet by consecutive action of multiple short intense laser pulses

X. WANG,[1] W. YU,[1,2] M.Y. YU,[2] V.K. SENECHA,[3] H. XU,[4] J.W. WANG,[1] X. YUAN,[5] AND Z.M. SHENG[7,6,2]

[1]Shanghai Institute of Optics and Fine Mechanics, Chinese Academy of Sciences, Shanghai, China
[2]Institute for Fusion Theory and Simulation, Zhejiang University, Hangzhou, China
[3]Raja Ramanna Centre for Advanced Technology, Indore, India
[4]School of Computer Science, National University of Defense Technology, Changsha, China
[5]School of Optoelectronic Science and Engineering, Huazhong University of Science and Technology, Wuhan, China
[6]Beijing National Laboratory of Condensed Matter Physics, Institute of Physics, Chinese Academy of Sciences, Beijing, China
[7]Department of Physics, Shanghai Jiao Tong University, Shanghai, China

(RECEIVED 4 July 2009; ACCEPTED 13 August 2009)

Abstract

The acceleration of a micrometer-sized plasma pellet at 100 critical densities (10^{23} cm^{-3}) by consecutive application of ultra-short ultra-intense laser pulses is studied using two-dimensional particle-in-cell simulation. It is shown that due to the repeated actions of the laser ponderomotive force, a small dense plasma pellet can be efficiently accelerated, with a considerable fraction of the plasma ions accelerated to high speeds. The proposed scheme can provide a high-density flux of energetic ions, which should be valuable in many practical applications.

Keywords: Ion bunch acceleration; PIC simulation; Short intense laser pulses

INTRODUCTION

The availability of ultra-short ultra-intense (USUI) laser pulses with peak intensities as high as 10^{21} Wcm^{-2} and contrast in excess of 10^8 (Liu *et al.*, 2009; McKenna *et al.*, 2008; Limpouch *et al.*, 2008; Nickles *et al.*, 2007; Ter-Avetisyan *et al.*, 2008; Karsch *et al.*, 1999; Malka & Fritzler, 2004; Koyama *et al.*, 2006) makes possible the development of compact laser-driven ion accelerators (Malka *et al.*, 2008; Krushelnick *et al.*, 2007; Mangles *et al.*, 2006). The resulting energetic ions have many important applications, ranging from medical proton therapy (Bulanov & Khoroshkov, 2002), diagnostics for laser-plasma interaction (MacKinnon *et al.*, 2004), and fast ignition in inertial-confinement fusion (Roth *et al.*, 2001). In most of these applications, energetic ions of sufficiently high energy and brightness are required.

Target normal sheath acceleration is one of the proposed schemes for ion acceleration (Wilks *et al.*, 2001; Allen *et al.*, 2003; Mora, 2003; Fuchs *et al.*, 2006). When an USUI laser pulse irradiates a solid foil, the relativistic electrons generated in the laser-plasma interaction can easily penetrate though the foil, and form an electron sheath on the rear side of the foil (Hegelich *et al.*, 2006; Schwoerer *et al.*, 2006; Yin *et al.*, 2008; Tian *et al.*, 2008), and the resulting space-charge field then pulls out plasma ions in the back surface. The energetic ions thus generated can be accelerated to several MeV (Hatchett *et al.*, 2000; Snavely *et al.*, 2000; Zepf *et al.*, 2003; Spencer *et al.*, 2003), but their density is rather low, usually <0.001 of the critical density.

In order to generate an energetic ion bunch of high density, the interaction of an USUI laser pulse with a small, dense plasma pellet was proposed (Yu *et al.*, 2005). In this scheme, a micrometer-sized plasma pellet is directly accelerated by a laser pulse of intensity exceeding 10^{21} Wcm^{-2} and densities exceeding 100 times the critical density (10^{23} cm^{-3}) can be achieved, with the total ion number in the plasma pellet above 10^{11}. It was shown by two-dimensional (2D) particle-in-cell (PIC) simulation that the plasma pellet can be accelerated to $v > 0.1c$, where c is the speed of light in vacuum. The kinetic energy of the ions in the core region of the plasma pellet can exceed 10 MeV at a density of 10^{21} Wcm^{-2}. The scheme has the additional advantage that, unlike the charged-particle beams, the energetic plasma pellet is essentially neutral.

For producing faster plasma pellets, more intense laser pulses are needed. However, it is not easy to increase the

Address correspondence and reprint requests to: Xin Wang, Shanghai Institute of Optics and Fine Mechanics, Chinese Academy of Sciences, Shanghai, China. E-mail: wxeverest@gmail.com

laser intensity to beyond 10^{21} Wcm^{-2}. As an alternative, we propose in this article, consecutive acceleration of the plasma pellet by a number of less-intense laser pulses. This multi-pulse scheme makes use of the repeated actions of the ponderomotive force, which dominates laser-target interactions (Yu *et al.*, 2007). It is expected to be more effective since weaker laser pulses are expected to suffer from less scattering and modulational instabilities during the laser-plasma interaction. Furthermore, as the plasma pellet is driven by the laser ponderomotive force several times, the interaction distance is enhanced since the later pulse act on an already speedy pellet, which keeps moving forward inertially during the interval between the pulses.

To see the effectiveness of the multi-pulse scheme, we first compare the results of pellet acceleration by a single and by two shorter laser pulses. The peak strength and total energy of the two shorter pulses are the same as that in the single pulse. It is found that the two-pulse scheme is indeed more efficient: in the same time interval, the plasma pellet is pushed forward a longer distance compared to that with a single-pulse, and *more* plasma ions are accelerated to *higher* speeds. To show that the plasma pellet can be further accelerated by applying more laser pulses, we also consider applying four laser pulses, with each pulse the same as that in the two-pulse case. It is verified that the additional laser pulses can further accelerate the plasma pellet. In fact, a considerable fraction of the pellet-plasma ions are accelerated to $>0.4c$, corresponding to an energy gain of 100 MeV. However, because of plasma expansion and laser-related perturbations, the resulting pellet occupies a somewhat larger volume. As expected, the ion density in the pellet core decreases, but it is still well above the critical density.

PIC SIMULATION

We performed 2D3V (two dimensional in space and three dimensional in velocity) PIC simulations (Xu *et al.*, 2002; Yu *et al.*, 2007) on the interaction of linearly polarized Gaussian laser pulses with a dense plasma pellet of micrometer size. The Gaussian laser pulses are incident along the x axis from the left vacuum region into the simulation box, as shown in Figure 1. The laser wavelength is $\lambda_0 = 1.06\ \mu$m, the normalized laser strength parameter is $a_L = 50$, and the laser spot size (diameter) is $d = 10\lambda_0$. The corresponding laser intensity is on the order of 10^{21} Wcm^{-2}. Thus, the electron motion is in the highly relativistic regime, and the laser ponderomotive force is dominant in the laser-plasma interaction. The pellet, of density $n_0 = 100n_c$, is initially $1\lambda_0$ in width and $1\lambda_0$ in thickness, and located in $9.5 < x/\lambda_0 < 10.5$ and $-0.5 < y/\lambda_0 < 0.5$, where $n_c = 10^{21}$ cm^{-3} is the critical density.

In the simulation, the computation box is $50\lambda_0 \times 20\lambda_0$, the spatial mesh contains 2000×800 cells, and each cell contains 625 ions and 625 electrons. The electron-ion mass ratio is $1/1836$, the initial velocity of the plasma electrons and ions are assumed to be Maxwellian with temperature

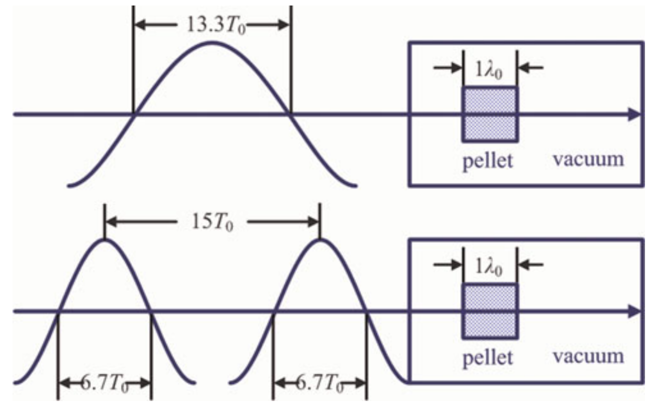

Fig. 1. (Color online) Schematic of simulations for comparison.

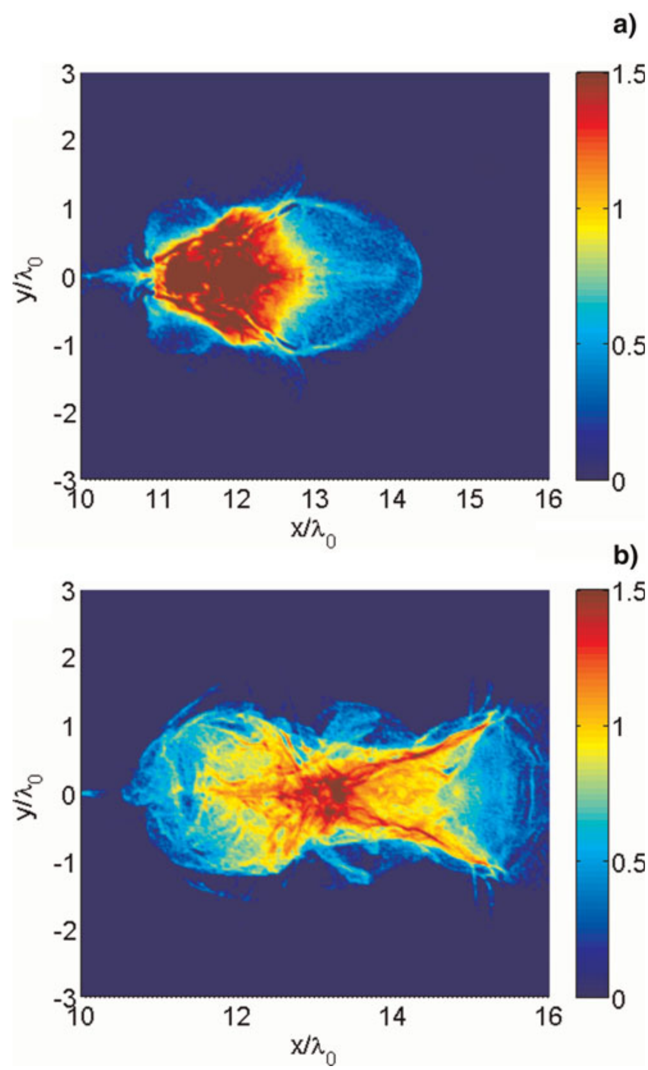

Fig. 2. (Color online) The ion density distribution at $t = 42T_0$ for the laser durations (**a**) $\tau = 13.3T_0$, and (**b**) $\tau = 6.7T_0$. Here T_0 is the laser period, $w = 5\lambda_0$ its spot radius, and $a_L = 50$ its strength parameter. The initial pellet (located at $9.5 < x/\lambda_0 < 10.5$) density is $n_0 = 100n_c$, its width is $1\lambda_0$, and its thickness is $1\lambda_0$. The color bars are for $\log(n_i/n_c)$.

https://doi.org/10.1017/S0263034609990371 Published online by Cambridge University Press

1 keV. The time step of the simulation is $0.016T_0$, where $T_0 \approx 3.5$ fs is the laser period. Absorbing boundaries are used for both the x and y simulation-box boundaries.

TWO-PULSE ACCELERATION

We begin with pellet acceleration by a single laser pulse of duration $\tau = 13.3T_0$. Figure 2a shows the plasma ion density at $t = 42T_0$, when the interaction with the laser pulse is over and the periphery of laser pulse has overtaken the plasma pellet (Yu *et al.*, 2005). One can see that the electrons as well as ions in the pellet are accelerated. We next consider pellet acceleration by two shorter laser pulses. Instead of a single pulse of $\tau = 13.3T_0$, we now use two $\tau = 6.7T_0$ pulses, each having the same parameters as that for Figure 2a, i.e., $a_L = 50$ and $w = 5\lambda_0$. The total energy in the two pulses is about the same as that in the single$13.3T_0$-pulse case. The time delay between the peaks of the two laser pulses is $15T_0$. Figure 2b shows the ion density at $t = 42T_0$, i.e., after interacting with the two laser pulses. Our result is similar to the experimental results of Kar *et al.* (2008). Therefore, the two-pulse acceleration scheme is more efficient: in the same period the plasma pellet is pushed forward a longer distance, compared to the single-pulse case.

In Figure 3, we compare the ion density distributions along the laser propagation axis ($y = 0$) for the plasma pellet accelerated by (a) a single $13.3T_0$ pulse, and (b) two $6.7T_0$ pulses. Figure 3a is for $t = 42T_0$, i.e., the same as in Figure 2a, and Figure 3b is for $t = 27T_0$ (black curve) and $42T_0$ (blue curve, online only), corresponding to instants when the non-focal-spot parts of the first and second laser pulses have both overtaken the plasma pellet. The distribution of the ion velocity along the laser propagation axis is shown in Figure 4a for the single-pulse case at $t = 42T_0$, and in Figure 4b for the two-pulse case at $t = 27T_0$ (black curve) and $42T_0$ (blue curve, online only). To show more clearly the difference between the two cases, we present in

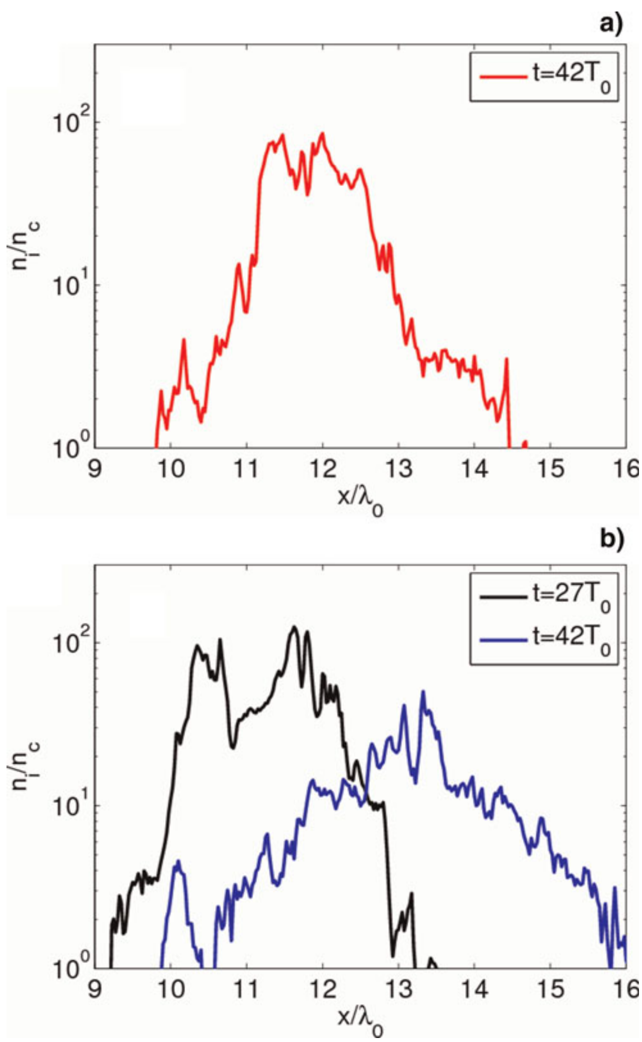

Fig. 3. (Color online) The ion density (normalized by n_c) variation along the laser propagation axis at (**a**) $t = 42T_0$, (**b**) $t = 27T_0$ and $42T_0$. The input parameters for the cases (a) and (b) are the same as that for Figures 2a and 2b, respectively.

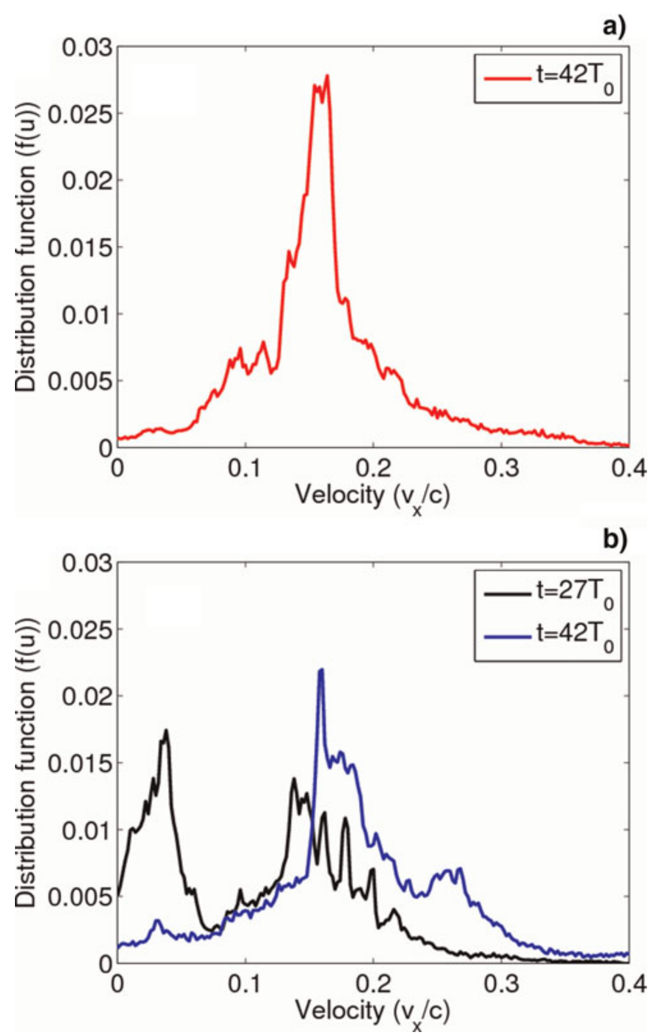

Fig. 4. (Color online) The ion velocity distribution functions along the laser propagation axis. (**a**) For $t = 42T_0$ and parameters same as that for Figure 2a. (**b**) For $t = 27T_0$ and $42T_0$, and parameters the same as that for Figure 2b.

Table 1. *The percentage of energetic ions whose velocities are higher than* $0.1c$, $0.2c$, $0.3c$ *and* $0.4c$, *where c is the light speed. The parameters used are the same as that for Figure* 2

t/T_0	u/c			
	>0.1	>0.2	>0.3	>0.4
42	84.19	19.55	3.84	0.26
27	47.60	9.49	1.00	0.00
42	82.89	35.08	5.79	0.77

Table 1 the percentage of the energetic ions (among all the pellet ions) whose velocities are higher than $0.1c$,$0.2c$,$0.3c$, and $0.4c$. The laser and plasma parameters are the same as that for Figures 2 to 4. We see that compared with that of the single laser pulse of the same peak intensity and total energy, the consecutive actions of two shorter pulses can push the plasma pellet forward more efficiently, with more plasma ions being accelerated to higher speeds. This result can be attributed to the repeated actions of the ponderomotive force on the pellet. In the two-pulse acceleration, the plasma pellet is pushed by laser ponderomotive force twice, and in the interval between the pulses the plasma pellet keeps moving forward inertially.

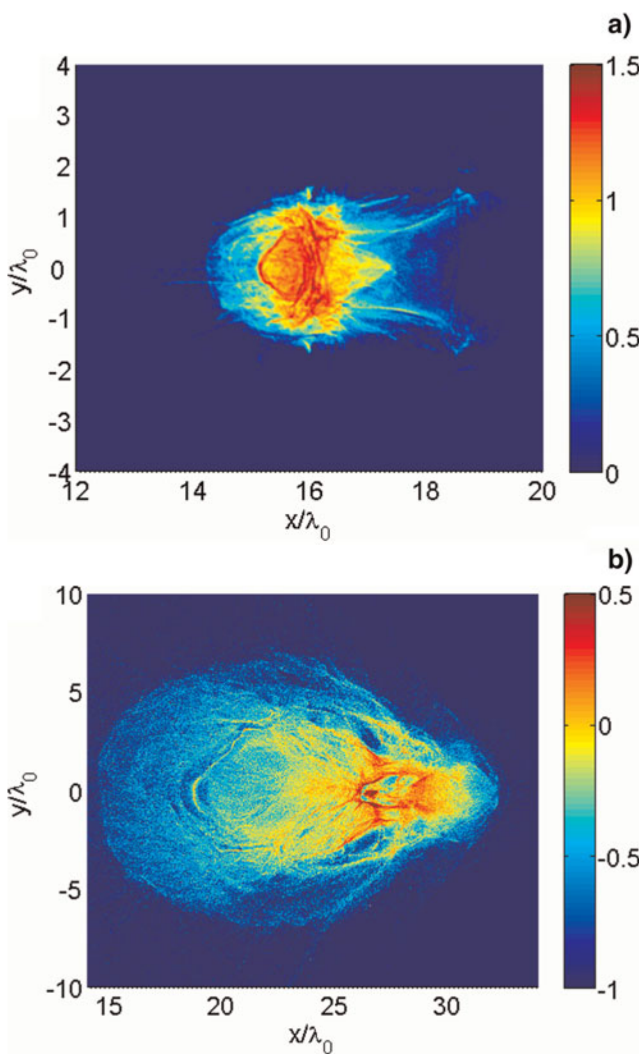

Fig. 5. (Color online) The ion density distribution at (**a**) $t = 48T_0$ and (**b**) $t = 72T_0$. Four laser pulses, each of $w = 5\lambda_0$, $a_L = 50$, $\tau = 6.7T_0$, and their peaks separated by $10T_0$, interact with the plasma pellet successively. The initial pellet parameters are the same as that for Figure 2. The color bars are for $\log(n_i/n_c)$.

MULTI-PULSE ACCELERATION

To see if the plasma pellet can be further accelerated if more laser pulses are used, we now apply four $\tau = 6.7T_0$ laser pulses at $10T_0$ intervals. The other parameters are the same as that of the two pulse case. Figure 5 shows the distribution of the ion density at $t = 48T_0$ and $72T_0$, corresponding to instants when the action of the third and the fourth pulses are over, respectively. Figures 6 and 7 shows the corresponding distributions of the ion density and velocity along the laser propagation direction. One can see that the additional laser pulses continuously push forward the plasma pellet, which now occupies a larger volume because of plasma expansion and laser-induced perturbations. As a result, the ion density at the core of the pellet decreases. Nevertheless, it is still well above the critical density. Table 2 shows the fractions of ions whose velocities are higher than $0.1c$, $0.2c$, $0.3c$, $0.4c$, $0.5c$, and $0.6c$. We note that a significant fraction ($>1/3$) of the ions in the pellet are accelerated to speeds $>0.4c$. The corresponding ion energy gain is up to 100 MeV.

CONCLUSION

In conclusion, we have investigated consecutive acceleration of a plasma pellet by a number of USUI laser pulses. We first compared the pellet acceleration by a single laser pulse with that by two shorter pulses of the same peak strength and total energy as the single pulse. It is shown that due to the repeated

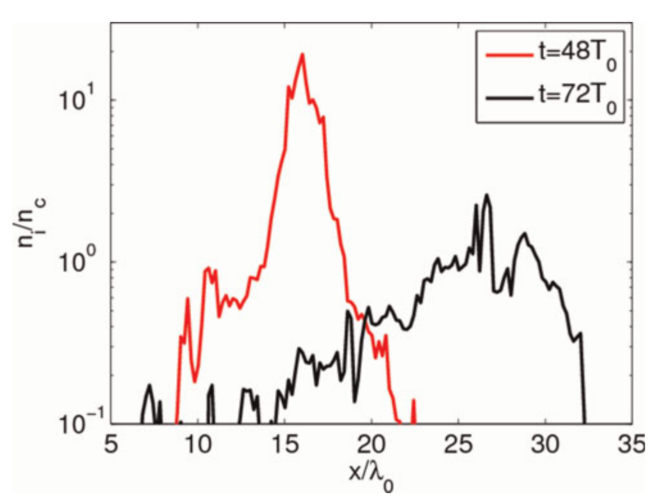

Fig. 6. (Color online) Variation of the ion density (normalized by n_c) along the laser propagation direction at $t = 48T_0$ and $72T_0$. The other parameters used are the same as that for Figure 5.

https://doi.org/10.1017/S0263034609990371 Published online by Cambridge University Press

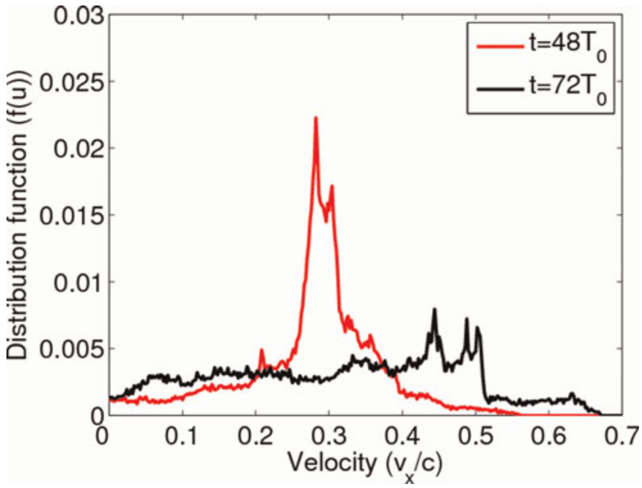

Fig. 7. (Color online) The ion velocity distribution along the laser propagation direction at $48T_0$ and $72T_0$. The other parameters used are the same as that for Figure 5.

Table 2. *The percentage of ions whose velocities are higher than* 0.1*c,* 0.2*c,* 0.3*c,* 0.4*c,*0.5*c and* 0.6*c, here c is light velocity. The parameters used are the same as that for Figure* 5

	u/c					
t/T_0	>0.1	>0.2	>0.3	>0.4	>0.5	>0.6
48	87.91	77.82	37.46	6.14	0.96	0.00
72	80.57	65.86	51.38	33.59	11.11	3.23

actions of the ponderomotive force, the two-pulse case is more efficient for pellet acceleration, with *more* plasma ions accelerated to *higher* speeds. We next considered the use of four laser pulses, with each pulse the same as that in the two-pulse case. It is found that the additional laser pulses can further accelerate the plasma pellet, with a considerable fraction of the plasma ions accelerated to energy gains of above 100 MeV. Because of plasma expansion and laser-related perturbations, the resulting plasma pellet occupies a larger volume, and the ion density in the pellet core is reduced from the initial value, although it is still well above the critical density (10^{21} cm^{-3}). This is in contrast to the ions produced by target-normal sheath acceleration and conventional charged-particle accelerators, where the typical density of the accelerated particles is considerably lower. The scheme here provides a higher flux of energetic ions, which is desirable in many real applications (Roth *et al.*, 2001; Bulanov & Khoroshkov, 2002; MacKinnon *et al.*, 2004; Mangles *et al.*, 2006; Krushelnick *et al.*, 2007; Malka *et al.*, 2008).

ACKNOWLEDGEMENTS

This work was supported by the Natural Science Foundation of China under Grant Nos. 10734130, 10775165, and 10835003, the Science and Technology Commission of Shanghai Municipality under Grant No. 08PJ14102, the National High-Tech ICF Committee of China, and National Basic Research Program of China (973 Program) under Grant Nos. 2007CB815101 and 2006CB806004, the united foundation of National Natural Science Foundation of China and Chinese Academy of Engineering Physics under Grant Nos. 10876011 and 10676010, Japan-Korea-China cooperative project on High Energy Density Sciences for Laser Fusion Energy, and the JSPS Japan-China Core University Program.

REFERENCES

Allen, M., Sentoku, Y., Audebert, P., Blazevic, A., Cowan, T., Fuchs, J., Gauthier, J.C., Geissel, M., Hegelich, M., Karsch, S., Morse, E., Patel, P.K. & Roth, M. (2003). Proton spectra from ultraintense laser–plasma interaction with thin foils: Experiments, theory, and simulation. *Phys. Plasmas* **10**, 3283.

Bulanov, S. & Khoroshkov, V. (2002). Feasibility of using laser ion accelerators in proton therapy. *Plasma Phys. Rep*. **28**, 453.

Fuchs, J., Antici, P., D'humières, E., Lefebvre, E., Borghesi, M., Brambrink, E., Cecchetti, C.A., Kaluza, M., Malka, V., Manclossi, M., Meyroneinc, S., Mora, P., Schreiber, J., Toncian, T., Pépin, H. & Audebert, P. (2006). Laser-driven proton scaling laws and new paths towards energy increase. *Nat. Phys*. **2**, 48.

Hatchett, S.P., Brown, C.G., Cowan, T.E., Henry, E.A., Johnson, J.S., Key, M.H., Koch, J.A., Langdon, A.B., Lasinski, B.F., Lee, R.W., Mackinnon, A.J., Pennington, D.M., Perry, M.D., Phillips, T.W., Roth, M., Sangster, T.C., Singh, M.S., Snavely, R.A., Stoyer, M.A., Wilks, S.C. & Yasuike, K. (2000). Electron, photon, and ion beams from the relativistic interaction of petawatt laser pulses with solid targets. *Phys. Plasmas* **7**, 2076.

Hegelich, B.M., Albright, B.J., Cobble, J., Flippo, K., Letzring, S., Paffett, M., Ruhl, H., Schreiber, J., Schulze, R.K. & Fernandez, J.C. (2006). Laser acceleration of quasi-monoenergetic MeV ion beams. *Nat*. **439**, 441–444.

Kar, S., Borghesi, M., Bulanov, S.V., Key, M.H., Liseykina, T.V., Macchi, A., Mackinnon, A.J., Patel, P.K., Romagnani, L., Schiavi, A. & Willi, O. (2008). Plasma jets driven by ultraintense-laser interaction with thin foils. *Phys. Rev. Lett*. **100**, 225004.

Karsch, S., Habs, D., Schatz, T., Schramm, U., Thirolf, P.G., Meyer-Ter-Vehn, J. & Pukhov, A. (1999). Particle physics with petawatt-class lasers. *Laser Part. Beams* **17**, 565–570.

Koyama, K., Adachi, M., Miura, E., Kato, S., Masuda, S., Watanabe, T., Ogata, A. & Tanimoto, M. (2006). Monoenergetic electron beam generation from a laser-plasma accelerator. *Laser Part. Beams* **24**, 95–100.

Krushelnick, K., Najmudin, Z. & Dangor, A.E. (2007). Particle acceleration using intense laser produced plasmas. *Laser Phys. Lett*. **4**, 847–862.

Limpouch, J., Psikal, J., Andreev, A.A., Platonov, K.Y. & Kawata, S. (2008). Enhanced laser ion acceleration from mass-limited targets. *Laser Part. Beams* **26**, 225–534.

Liu, M.P., Xie, B.S., Huang, Y.S., Liu, J. & Yu, M.Y. (2009). Enhanced ion acceleration by collisionless electrostatic shock in thin foils irradiated by ultraintense laser pulse. *Laser Part. Beams* **27**, 327–333.

MacKinnon, A.J., Patel, P.K., Town, R.P., Edwards, M.J., Phillips, T., Lerner, S.C., Price, D.W., Hicks, D., Key, M.H., Hatchett, S., Wilks, S.C., Borghesi, M., Romagnani, L., Kar, S., Toncian, T., Pretzler, G., Willi, O., Koenig, M., Martinolli, E., Lepape, S., Benuzzi-Mounaix, A., Audebert, P., Gauthier, J.C., King, J., Snavely, R., Freeman, R.R. & Boehlly, T. (2004). Proton radiography as an electromagnetic field and density perturbation diagnostic. *Rev. Sci. Instrum*. **75**, 3531.

Malka, V. & Fritzler, S. (2004). Electron and proton beams produced by ultra short laser pulses in the relativistic regime. *Laser Part. Beams* **22**, 399–405.

Malka, V., Faure, J., Gauduel, Y.A., Lefebvre, E., Rousse, A. & Phuoc, K.T. (2008). Principles and applications of compact laser-plasma accelerators. *Nat. Phys*. **4**, 447–453.

Mangles, S.P.D., Walton, B.R., Najmudin, Z., Dangor, A.E., Krushelnick, K., Malka, V., Manclossi, M., Lopes, N., Carias, C., Mendes, G. & Dorchies, F. (2006). Table-top laser plasma acceleration as an electron radiography source. *Laser Part. Beams* **24**, 185–190.

McKenna, P., Carroll, D.C., Lundh, O., Nurnberg, F., Markey, K., Bandyopadhyay, S., Batani, D., Evans, R.G., Jafer, R., Kar, S., Neely, D., Pepler, D., Quinn, M.N., Redaelli, R., Roth, M., Wahlstrom, C.G., Yuan, X.H. & Zepf, M. (2008). Effects of front surface plasma expansion on proton acceleration in ultraintense laser irradiation of foil targets. *Laser Part. Beams* **26**, 591–596.

Mora, P. (2003). Plasma expansion into a vacuum. *Phys. Rev. Lett*. **90**, 185002.

Nickles, P.V., Ter-Avetisyan, S., Schnuerer, M., Sokollik, T., Sandner, W., Schreiber, J., Hilscher, D., Jahnke, U., Andreev, A. & Tikhonchuk, V. (2007). Review of ultrafast ion acceleration experiments in laser plasma at Max Born Institute. *Laser Part. Beams* **25**, 347–363.

Roth, M., Cowan, T.E., Key, M.H., Hatchett, S.P., Brown, C., Fountain, W., Johnson, J., Pennington, D.M., Snavely, R.A., Wilks, S.C., Yasuike, K., Ruhl, H., Pegoraro, F., Bulanov, S.V., Campbell, E.M., Perry, M.D. & Powell, H. (2001). Fast ignition by intense laser-accelerated proton beams. *Phys. Rev. Lett*. **86**, 436.

Schwoerer, H., Pfotenhauer, S., Jackel, O., Amthor, K.-U., Liesfeld, B., Ziegler, W., Sauerbrey, R., Ledingham, K.W.D. & Esirkepov, T. (2006). Laser-plasma acceleration of quasi-monoenergetic protons from microstructured targets. *Nat*. **439**, 445–448.

Snavely, R.A., Key, M.H., Hatchett, S.P., Cowan, T.E., Roth, M., Phillips, T.W., Stoyer, M.A., Henry, E.A., Sangster, T.C., Singh, M.S., Wilks, S.C., Mackinnon, A., Offenberger, A., Pennington, D.M., Yasuike, K., Langdon, A.B., Lasinski, B.F., Johnson, J., Perry, M.D. & Campbell, E.M. (2000). Intense high-energy proton beams from petawatt-laser irradiation of solids. *Phys. Rev. Lett*. **85**, 2945.

Spencer, I., Ledingham, K.W.D., Mckenna, P., Mccanny, T., Singha, R.P., Foster, P.S., Neely, D., Langley, A.J., Divall, E.J., Hooker, C.J., Clarke, R.J., Norreys, P.A., Clark, E.L., Krushelnick, K. & Davies, J.R. (2003). Experimental study of proton emission from 60-fs, 200-mJ high-repetition-rate tabletop-laser pulses interacting with solid targets. *Phys. Rev. E* **67**, 046402.

Ter-Avetisyan, S., Schnurer, M., Polster, R., Nickles, P.V. & Sandner, W. (2008). First demonstration of collimation and monochromatisation of a laser accelerated proton burst. *Laser Part. Beams* **26**, 637–642.

Tian, Y.W., Yu, W., Lu, P.X., Xu, H., Senecha, V.K., Lei, A.L., Shen, B.F. & Wang, X. (2008). Generation of periodic ultrashort electron bunches and strongly asymmetric ion Coulomb explosion in nanometer foils interacting with ultra-intense laser pulse. *Phys. Plasmas* **15**, 053105.

Wilks, S.C., Langdon, A.B., Cowan, T.E., Roth, M., Singh, M., Hatchett, S., Key, M.H., Pennington, D., Mackinnon, A. & Snavely, R.A. (2001). Energetic proton generation in ultra-intense laser–solid interactions. *Phys. Plasmas* **8**, 542.

Xu, H., Chang, W.W., Zhuo, H.B., Chang, L.H. & Yue, Z.W. (2002). Parallel programming of 2(1/2)-dimensional PIC underdistributed-memory parallel environments. *Chin. J. Comput. Phys*. **19**, 305.

Yin, Y., Yu, W., Yu, M.Y., Lei, A.L., Yang, X.Q., Xu, H. & Senecha, V.K. (2008). Influence of target thickness on the generation of high-density ion bunches by ultrashort circularly polarized laser pulses. *Phys. Plasmas* **15**, 093106.

Yu, W., Xu, H., He, F., Yu, M.Y., Ishiguro, S., Zhang, J. & Wong, A.Y. (2005). Direct acceleration of solid-density plasma bunch by ultraintense laser. *Phys. Rev. E* **72**, 046401.

Yu, W., Yu, M.Y., Xu, H., Tian, Y.W., Chen, J. & Wong, A.Y. (2007). Intense local plasma heating by stopping of ultrashort ultraintense laser pulse in dense plasma. *Laser Part. Beams* **25**, 631–638.

Zepf, M., Clark, E.L., Beg, F.N., Clarke, R.J., Dangor, A.E., Gopal, A., Krushelnick, K., Norreys, P.A., Tatarakis, M., Wagner, U. & Wei, M.S. (2003). Proton Acceleration from High-Intensity Laser Interactions with Thin Foil Targets. *Phys. Rev. Lett*. **90**, 064801.